Characterization of patient-specific biventricular mechanics in heart failure with preserved ejection fraction: hyperelastic warping*

Hua Zou, Xiaodan Zhao, Xi Ce, Lik Chuan Lee, Martin Genet, Yi Su, Rusan Tan, and Liang Zhong, *Member, IEEE*

Abstract— **Heart failure with preserved ejection fraction (HFPEF) is considered as a major public health problem. Traditionally, HFPEF is diagnosed based on a "normal" EF, but the studies have explored the potential role of left ventricular mechanics. Furthermore, right ventricular mechanics and bi-ventricular interaction in HFPEF is currently not well understood. In this study, we aim to develop a framework using a hyperelastic warping approach to quantify bi-ventricular and septum strains from cardiac magnetic resonance (CMR) images. Whole heart models were reconstructed in HFPEF, HF with reduced EF (HFREF) and normal control patients, and a Laplace-Dirichlet Rule-Based (LDRB) algorithm was employed to assign circumferential orientation. The LV circumferential strain was 10.56% in normal control, and decreased to 5.90% in HFPEF and 1.66% in HFREF. Interestingly, the RV circumferential strain was 7.29% in normal control, but increased to 8.93% in HFPEF, and decreased to 2.16% in HFREF. The septum circumferential strain was comparable between HFPEF and normal control. Heart failure with preserved ejection fraction demonstrated augmented right ventricular strain and comparable septum strain to maintain its "normal" ejection fraction. This might unveil a new mechanism of bi-ventricular interaction and compensation in heart failure with preserved ejection fraction.**

I. Introduction

Heart failure (HF) imposes major global health care burden on the society and inflicts suffering on the individual [1]. In the US, HF affects 5.7 million patients, and is the major cause of hospitalization for people over 65 years with 25% to 50% rate of hospitalization [2]. The disease prevalence continues to escalate with the aging of population. Impaired pump function, expressed as a reduced left ventricular ejection fraction (EF), is frequently used as a marker of HF (HF with reduced EF). However, about 30-50% of HF patients have preserved EF[3-5]. HFPEF patients are typically older women who owned the history of hypertension, but carries similar mortality as HFREF. In this situation, more intricate bi-ventricular deformation and mechanics assessment may be necessary to characterize HFPEF.

Recent studies have demonstrated the potential existence of abnormalities of LV strain, strain rate, torsion and asynchrony by using echocardiography, despite its "normal" LVEF in HFPEF [6]. However, echocardiography is operator-dependent and suffers from poor inter-study reproducibility [7]. Furthermore, studies on the right ventricular and ventricular septum deformation and mechanics in HFPEF are very limited. Cardiac magnetic resonance (CMR) images provide superior resolution and reproducible results, to quantify ventricular curvedness, deformation, systolic and diastolic function in diverse heart diseases [8-11] as well as validating computational models [12-13].

In this study, we aimed to i) develop a hyperelastic wrapping approach to quantify left ventricle, right ventricular and ventricular septum deformation in terms of circumferential strain, and ii) characterize the abnormalities in circumferential strain in HFPEF patients in comparison with HFREF and normal control patients.

The organization of the paper is as follows: Section 2 states the method to analyze the circumferential strains of LV, RV and septum by using hyperelastic wrapping approach. In Section 3, the circumferential strains for HFPEF, HFREF and normal control are presented and compared. Discussions are also given in this section. Section 4 presents the conclusions of the study.

II. Method

In this study, the platform was tested on age-comparable and gender-matched HFPEF, HFREF and normal control. Approval was obtained from the Singhealth Centralised Institutional Review Board for human research, and informed consents are given by all enrolled participates.

A. Procedures

A 3T Philips scanner was used to obtain cine MR images with ECG gating where the acquisition was performed for both long- and short-axes. The proposed post-imaging processing method includes the following steps (see Fig. 1): (1) Image acquisition; (2) Contour delineation; (3) Surface generation; (4) Mesh generation; (5) Material region partition; (6) Fibre orientation assignment; (7) Deformable image registration; (8) Circumferential strain calculation. Among which, the contour delineation and surface generation

* Research supported in part by grants from the Biomedical Engineering Programme, Agency for Science, Technology and Research, Singapore Project Grant (132 148 0012), and the Biomedical Research Council (14/1/32/24/002) and Goh Cardiovascular Research Grant (DUKE-NUS/GCR/2013/0009).

H.Z. XDZ, RST and LZ are with National Heart Centre Singapore, 5 Hospital Drive, 169609 Singapore (corresponding author: 6567042237; e-mail: zhong.liang@nhcs.com.sg).

X.C and L.C.L are from Michigan State University, East Lansing, MI, United States

M.G is from École Polytechnique, Paris

Y.S is from Institute of High Performance Computing, A*STAR

were divided into LV, RV and epicardium regions. An example of strain calculation is shown in Fig. 2.

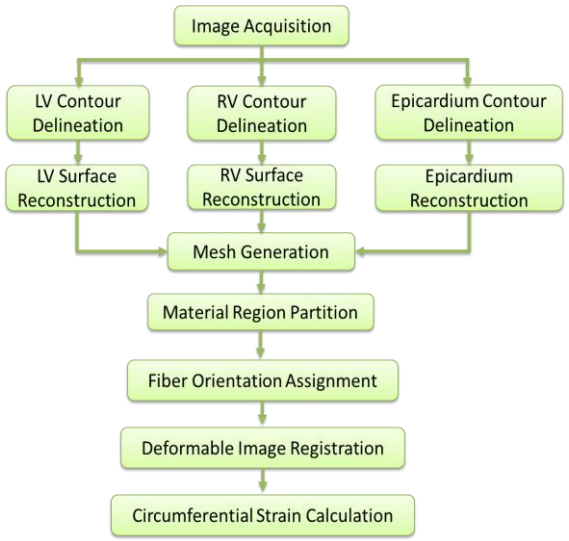

Fig. 1. Flow chart to calculate the circumferential strain

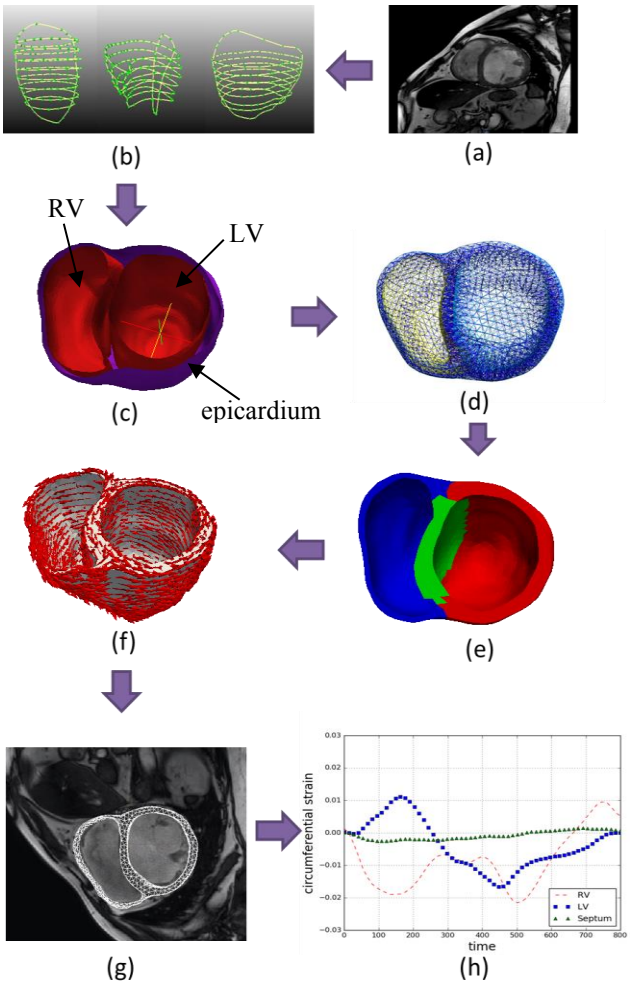

Fig. 2. Practical procedures involved in obtaining the circumferential strain. (a) MR images. (b) Contours for LV, RV and Epicardium. (c) Generated surface. (d) Generated mesh. (e) Partition of LV, RV and septum regions. (f) Assigned fiber orientation. (g) Hyperelastic warping. (h) Circumferential strain curves for RV, LV and Septum.

B. Hyperelastic warping

Hyperelastic warping is a technique employed for deformable registration between images. In this method [14], a finite element (FE) representation of the template image (T) is constructed and then deformed to align with the target image (S) during the registration process [15]. Let the deformation map be $\varphi(\mathbf{X}) = \mathbf{x} = \mathbf{X} + \mathbf{u}(\mathbf{X})$, where $\mathbf{x}$ is the current position, $\mathbf{X}$ is the reference position and $\mathbf{u}$ is the displacement. The Green-Lagrangian strain tensor is used, which is given as

$$\varepsilon = \frac{1}{2}(F + F^T + F^T F) \tag{1}$$

where $F(\mathbf{X}) = \partial\varphi(\mathbf{X})/\partial\mathbf{X}$ is the deformation gradient.

The energy function E is given by [11]

$$\mathrm{E}(\varphi) = \int_\beta \mathrm{W}(\mathrm{X},\varphi)\frac{\mathrm{dv}}{\mathrm{J}} + \int_\beta \mathrm{U}(\mathrm{T}(\mathrm{X},\varphi),\mathrm{S}(\mathrm{X},\varphi))\frac{\mathrm{dv}}{\mathrm{J}} \tag{2}$$

where W is the hyperelastic strain energy term to regularize the deformation map, and U is an image energy density functional based on the image data in the template and target images and can be represented as:

$$U(\boldsymbol{X},\varphi) = \frac{\lambda}{2}\big(T(\boldsymbol{X},\varphi) - S(\boldsymbol{X},\varphi)\big)^2 \tag{3}$$

where λ is the penalty parameter that enables the alignment of the template model with target images. By minimizing the energy function, the strain is generated through the deformation from the template image to the target image.

C. Fiber orientation assigning

A Laplace-Dirichlet Rule-Based (LDRB) algorithm is employed to assign the circumferential direction in the heart model. Detailed information of this algorithm is described in [16]. To do so, the fiber distributions for the models in this paper are defined as 0° epicardial to 0° endocardial, as shown in Fig. 2 (f).

III. RESULTS

The proposed program was more about a framework with limited cases (one HFREF, one HFPEF and one normal control). It was successfully experimented on the HFREF, HFPEF and normal control patients. The baseline characteristics of subjects and peak circumferential results are shown in Table. The three-dimensional heart models, regions and circumferential strain curves are shown as Fig. 3~5.

As expected, HFREF presented dilated ventricles (LVEDV of 479 ml and RVEDV of 264 ml) and reduced bi-ventricular ejection fraction (LVEF of 8% and RVEF of 16%). The circumferential strains in LV, RV and septum are significantly reduced, as shown in Fig. 3. Interestingly, the circumferential strain curve demonstrated that there was possible untwist deformation at early systolic phase, which may due to the residual stress in the heart.

The HFPEF patient has a slight bigger left ventricle (LVEDV of 245 ml), but smaller right ventricle (RVEDV of 160 ml), and preserved bi-ventricular ejection fraction (LVEF of 43% and RVEF of 49%), in comparison with normal control. LV strain decreased, septum strain was comparable,

but RV strain increased surprisingly and is more than the normal control. This may be due to the RV compensatory mechanism to maintain the preserved pumping function (i.e., preserved ejection fraction).

The normal subject demonstrated that circumferential strain decreased from LV, RV to septum (LV: 10.56%; RV: 7.29% and Septum: 5.18%). While HFPEF has shown that RV had biggest strain, following by the LV and then septum (see Fig. 6). Future prospective studies in large cohort are needed to validate this interesting mechanism in HFPEF.

TABLE I. PATIENT INFORMATION AND CIRCUMFERENTIAL STRAINS.

	HFREF (LVEF=8%)	HFPEF (LVEF=43%)	CON (LVEF=65%)
Age, years	50	54	57
Gender	Male	Male	Male
Weight, kg	93	105	73
Height, cm	167	171	171
Body mass index, kg/m^2	33.3	36	25
Body surfaced area, m2	2.02	2.16	1.86
Systolic blood pressure, mmHg	111	118	145
Diastolic blood pressure, mmHg	67	66	92
LV end-diastolic volume, ml	479	245	157
LVend-systolic volume, ml	440	141	55
LV stroke volume, ml	39	105	102
LV ejection fraction, %	8	43	65
LV mass, g	246	135	94
RVend-diastolic volume, ml	264	160	186
RV end-systolic volume, ml	222	82	92
RV stroke volume, ml	41	78	94
RV ejection fraction, %	16	49	50
LVPCS, %	1.66%	5.90%	10.56%
RVPCS, %	2.16%	8.93%	7.29%
SeptumPCS, %	2.47%	4.52%	5.18%

LVPCS: Left ventricle peak circumferential strain; RVPCS: Right ventricle peak circumferential strain; SeptumPCS: Septum peak circumferential strain.

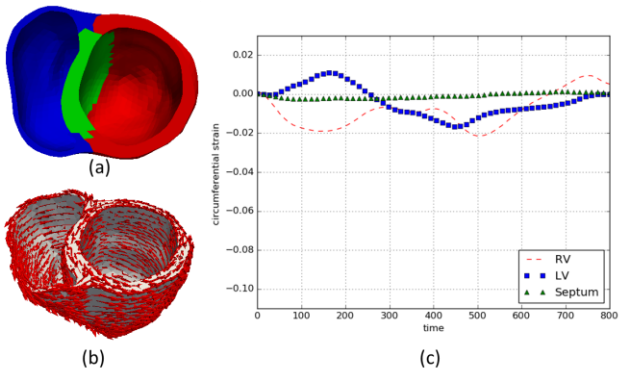

Fig. 3. Results for HFREF. (a) Region partition (LV, RV, Septum). (b) Heart model with assigned fiber orientation. (c). Circumferential strain curves (LV, RV, Septum). The peak strain in LV, RV and septum are 1.66%, 2.16% and 2.47%.

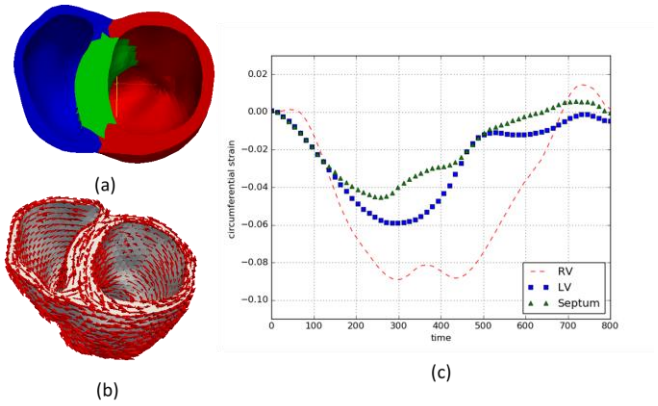

Fig. 4. Results for HFPEF. (a) Region partition (LV, RV, Septum). (b) Heart model assigned with fiber orientation. (c). Circumferential strain curves (LV, RV, Septum). The peak strain in LV, RV and septum are 5.90%, 8.93% and 4.52%.

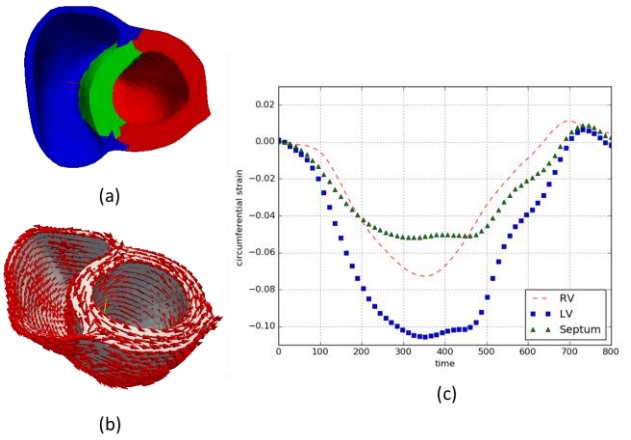

Fig. 5. Results for normal control. (a) Region partition (LV, RV, septum). (b) Heart model assigned with fiber orientation. (c). Circumferential strain curves (LV, RV, Septum). The peak strain in LV, RV and septum are 10.56%, 7.29% and 5.18%.

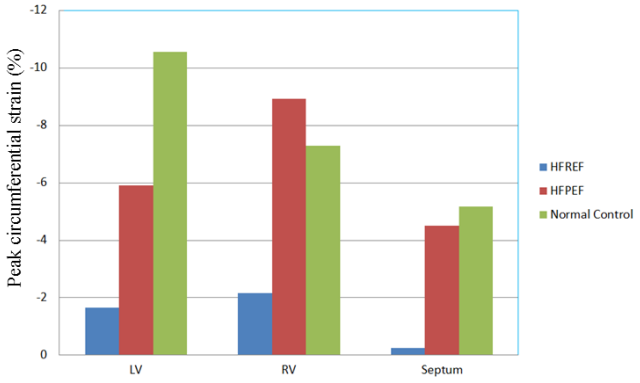

Fig. 6. Peak circumferential strains for LV, RV and Septum in HFREF, HFPEF and normal control.

IV. CONCLUSION

We presented a framework to calculate circumferential strain, in the bi-ventricles and septum in a one stop-shop hyperelastic wrapping approach from cardiac magnetic resonance images. Heart failure with preserved ejection

fraction demonstrated augmented right ventricular strain and comparable septum strain, despite decreased left ventricular strain. This might unveil a new mechanism of bi-ventricular interaction and compensation in heart failure with preserved ejection fraction.

V. REFERENCES

[1] A. S. Hunt. ACC/AHA 2005 guideline update for diagnosis and management of chronic heart failure in the adult: a report of the American College of Cardiology/American Heart Association Task Force on Practice Guidelines (Writing Committee to Update the 2001 Guideline for the Evfaluation and management of Heart Failure). J Am Coll Cardiol 2005;46:e1-82.

[2] Heart Disease and Stroke Statistics-2004 Update. Dellas, Tex: American Heart Association; 2004;

[3] S. Neubauer. The failing heart - an engine out of fuel. N Engl J Med 2007;356:1140-1151.

[4] K. Hogg, K. Swedberg, J. McMurray. Heart faiure with preserved left ventricular systolic function: epidemiology, clinical characteristics, and prognosis. J Am Coll Cardiol 2004;43:317-327.

[5] A. Ahmed, M. W. Rich, J. L. Fleg, M. R. Zile, J. B. Young, D. W. Kitzman. Effects of digosin on morbidity and mortality in diastolic heart failure: the ancillary digitalis invesigation group gril. Circulation 2006;114:397-403.

[6] J. Wang, S. F. Nagueh. Current perspective on cardiac function with diastolic heart failure. Circulation 2009;119:1146-1157.

[7] N. G. Bellenger, M. I. Burgess, S. G. Ray. Comparison of left ventricular ejection fraction and volumes in heart failure by echocardiography, radionuclide ventriculography and cardiovascular magnetic resonance; are they interchangeable? Eur Heart J 2000;21:1387-1396.

[8] L. Zhong, Y. Su, S. Y. Yeo, *et al*. Left ventricular regional wall curvedness and wall stress in patients with ischemic dilated cardiomyopathy. *Am J Physiol Heart Circ Physiol* 2009; 296:H573-H584.

[9] L. Zhong, Y. Su, L. Gobeawan L, et al. Impact of surgical ventricular restoration on ventricular shape, wall stress and function in heart failure paitents. *Am J Physiol Heart Circ Physiol* 2011; 300(5):H1653-1660.

[10] L. Zhong, L. Gobeawan, Y. Su, et al. Right ventricular regional wall curvedness and area strain in patients with repaired tetralogy of Fallot. *Am J Physiol Heart Circ Physiol* 2012; 302(6):H1306-H1316.

[11] S. Leng, X. Zhao, F. Q. Huang, J Wong, B. Su, J.C. Allen, G. Kassab, RS Tan, L. Zhong. Automated quantitative assessment of cardiovascular magnetic resonance - derived atrioventricular junction velocities. *Am J Physiol Heart Circ Physiol* 2015; 309(11):H1923-H1935.

[12] L. Lee, M. Genet, A. Dang, et al. Application of computational modeling in cardiac surgery. *Journal of cardiac surgery* 2014; 29(3):293-302.

[13] M. Genet, L. Lee, R. Nguyen, et al. Distribution of normal human left ventricular myofiber stress at end diastole and end systole: a target for in silico design of heart failure treatments. *Journal applied physio* 2014, 114(2):142-152.

[14] M. Genet, C. Stoeck, C. Von Deuster, et al. Finite element digital image correlation of whole-heart tagged and non-tagged images for cardiac strain analysis: possibility and limits. (In preparation).

[15] A. I. Veress, G. T. Gullberg, and J. A. *Weiss, "Measurement of strain in the left ventricle with cine-MRI and deformable image registration," *J. Biomech. Eng.*, vol. 127, no. 7, pp. 1195–1207, 2005.

[16] J. D. Bayer, R. C. Blake, G. Plank, and N. A. Trayanova, "A Novel Rule-Based Algorithm for Assigning Myocardial Fiber Orientation to Computational Heart Models," *Ann. Biomed. Eng.*, vol. 40, no. 10, pp. 2243–2254, Oct. 2012.